ENGINEERING RESEARCH JOURNAL (ERJ)
Vol. 1, No. 50 October 2021, pp.93-105
Journal Homepage: erj.bu.edu.eg

Shear Performance of Steel Fibers Lightweight RC Deep Beams: Numerical and Analytical Study

Mohamed S. Manharawy[1], Ahmed A. Mahmoud[2], Osama O. El-Mahdy[2], Mosaad H. El-Diasity[2]
[1]Higher Institute of Engineering, 15th of May City, Egypt
[2] Civil Engineering Dept., Faculty of Engineering, Shoubra, Benha University

Abstract : This paper aims to study numerically and analytically the effect of steel fibers on the behavior of reinforced lightweight concrete (RLWC) deep beams using strut and tie model (STM) and ANSYS program. The effect of nine parameters on the behavior: (1) effect of concrete compressive strength f_{cu}; (2) effect of yield reinforcing steel strength f_y; (3) effect of beam depth; (4) effect of beam width; (5) effect of shear span to depth ratio (a/d); (6) effect of main steel ratio; (7) effect of web reinforcement; (8) effect of fiber content and (9) effect of fiber aspect ratio are studied. The experimental results carried out by Manharawy [1] are verified using STM and ANSYS 15 computer program. The performance of RLWC deep beams was investigated in terms of: (1) cracking load; (2) cracking pattern; (3) ultimate load; (4) failure mode; (5) displacement ductility and (6) toughness. It is concluded that both the Egyptian code ECP-2017 [2] and ACI code 318-18 [3] are conservative in calculating the ultimate shear for RLWC deep beams.

Keywords: Reinforced lightweight concrete; deep beams; steel fibers; numerical; strut and tie model; ANSYS program.

1. Introduction

The analysis of reinforced concrete deep beams according to ECP 203-2017 [2] and ACI 318-18 [3] by strut and tie method (STM) is widely used. According to ACI 318-19 [3] design guide, deep beam is at least one of the following conditions:

i. Regions with concentrated loads are within twice the member depth from the face of the support; and
ii. Clear span is equal to or less than four times the deep beam depth.

Lightweight concrete (LWC), could be used for structural purpose after enhancing its performance in tension by using fibers [4, 5]. LWC has the following properties in addition to its light weight: (1) high thermal insulation properties; (2) flow ability; (3) self-compacting; and (4) speed of construction [6, 7]. The behavior of deep beams requires special considerations in experiment work, analysis and design, in addition to detailing of reinforcement [8 - 10]. Steel fibers in lightweight concrete increases the flexural and tensile strength, resistance to dynamic and sudden loading and strength against explosive effects [10-13].

Magdalene and Kanmani [15], verify the experimental study of (M20 grade) deep beam with different span to depth ratios (1.5, 2.0 and 2.5), and used ANSYS 9.0 to analyze the results. Many researchers have studied deep beams and come out with their design method, using STM [17- 22].

STM is used in this paper according to ECP 203-2017 [2] and ACI 2018-18 [3] with standard specific condition span-to-total-depth ratio ($L/t < 2$) for simply supported deep beam, where effective span is given by lesser of the following values:

(a) 1.15 times the clear span (L_0); and
(b) Center-to center (C/C) distance between the supports.

Researchers [22, 23] studied the nonlinear behavior of deep beams using ANSYS program and concluded that this program can predict the behavior in a good accuracy. Researchers [24-26] studied analytically the behavior of deep beams using different methods.

2.Strut and Tie Method (STM)

STM is used to design of disturbed region (D-regions) were plane section remaining plane before and after bending does not hold true. As shown in Figure 1. The angle between the axes of struts and tie is (θ) should be as large as possible to avoid incompatibilities and reduce cracking due to shortening of strut and lengthen of the tie occurring otherwise in almost the same direction.

$$\theta = tan^{-1}\left(\frac{h - c_1 - c_2}{a}\right) \quad (1)$$

The angle (Θ) should be not less than 26° according to ECP 203-2017 code [2] or equal 25° according to ACI 318-18[3].
where:

a: is the shear span measured from center lines between the load and support bearing plate.
h: is the beam total depth.
c_1: is the concrete cover distance from the top steel bars to the top beam surface.
c_2: is the concrete cover distance from the bottom longitudinal steel bars to the beam soffit.
The diagonal struts ($F_{u,\ AB}$, $F_{u,CD}$) and the compressive force in horizontal top strut ($F_{u,BC}$) are given by

The diagonal struts ($F_{u,\ AB}$, $F_{u,CD}$) and the compressive force in horizontal top strut ($F_{u,BC}$) are given by

$F_{u,BC} = f_{cd1} \cdot A_{str1}$ (2)
$F_{u,AB} = f_{cd2} \cdot A_{str2b}$ (for nodal zone A) (3)
$F_{u,AB} = f_{cd2} \cdot A_{str2t}$ (for nodal zone B) (4)

The compression capacity of strut (F_c) can be determined depending on the shape of strut and it can be calculated generally as:
$F_c = f_{cd} \cdot A_{str}$ (5)
where:
f_{cd1}, f_{cd2}, and f_{cd}: are the effective compressive strength of fibrous concrete strut at the strut under consideration;
A_{str1} , A_{str2} *and* A_{str} : are the cross-sectional area of the strut at the strut end under consideration.
For tapered strut
$f_{cd2} = z.\beta_{nf}.f_{cuf}$ (6)
It is taken as the smaller of (f_{cd1}) and (f_{cd2})
where:
z : is the coefficient depends on the design code, equal 0.67 for Egyptian code ECP 203-2017[2];
β_{nf} : is the nodal zone stress condition factor of fibrous concrete; and
f_{cuf} :is the compressive strength of the fibrous concrete
$f_{cuf} = f_{cu}\ (1+ 0.1066\ F)$ (7)

$$F = \frac{V_f\, l_f}{\phi_f} \quad (8)$$

where:
f_{cu} : is the concrete cubic compressive strength without fibers;
F: is the fiber factor;
V_f : is the fiber content ratio;
l_f : is the fiber length; and
ϕ_f :is the fiber diameter.
For prismatic strut: It is taken as (f_{cd1})
$f_{cd1} = z.\ \beta_{sf}.\ f_{cuf}$ (9)

As shown in Figure 1, a simply supported deep beam with nodal zone (A and B) is identified according to STM. Nodal zone (A) at the support is (C-C-T) type and nodal zone (B) is (C-C-C) type. From equilibrium conditions:

$$T = F_{u,AD} = \frac{V_u}{\tan\theta} \quad \text{(Force in the composite tie)} \qquad (10.a)$$

$$C = F_{u,BC} = \frac{V_u}{\tan\theta} \quad \text{(Forec in the compressed top strut)} \qquad (10.b)$$

$$F_{u,AD} = n_s .[(f_y.A_{bar}) + \sigma_{pc} ((w_{ct})^2 - A_{bar})] \qquad (11)$$

By using equation (11) and substitute in equation (12)

$$V_{u(1)} = n_s . \left[(f_y \times A_{bar}) + \sigma_{pc} ((w_{ct})^2 - A_{bar})\right] \tan\theta \qquad (12)$$

While by using equation (10.b) and substitute in equation (13)

$$F_{u,BC} = z.\beta_{sf}.f_{cuf} . b. w_s \qquad (13)$$

$$V_{u(2)} = [0.67.\beta_{sf}. f_{cuf} . b. w_s]. \tan\theta \qquad (14)$$

The value of shear capacity is the smaller of V_{u1} or V_{u2}.

where:

n_s: is the number of main bottom bars adopted for tension steel;

f_y: is the yielding strength of the steel bars;

A_{bar}: is the post-cracking tensile of fibrous concrete strength;

b: is the beam width; and

V_{u1}, V_u2 and V_{u3} are the ultimate shear forces.

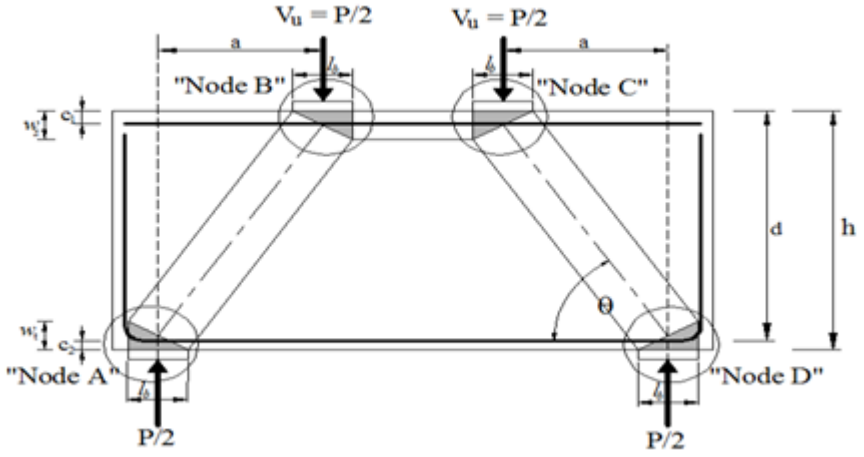

Fig 1 Strut and tie modeling

3.Nonlinear Finite Element Analysis

In this study, nonlinear structural analysis program ANSYS V15 is used to create numerical simulation. To verify the used model, a verification model of NSSFRC deep beam which experimentally tested by Adam et al [27] was used as shown in Figure 2. Figure 3 shows the load deflection relation between the numerical and the experimental curve of tested beam.

Eight-nodes solid element (SOLID 65) is used for modeling concrete as shown in Figure 4.a, with three translational degrees of freedom (X, Y and Z directions) at each node. Special features of SOLID 65 are taken into consideration such as: plasticity, cracking, creep, large strain and large deflection and also capable of plastic deformation. The used size of the mesh to model the beams is 25mmx25mmx25 mm. Link- 8 element was used to model the steel reinforcement as shown in Figure 4.b. It has two nodes with three degrees of freedom-translations at each node at X, Y and Z directions. The numerical program consists of four groups; each group has two beams in addition to the control specimen. All deep beams have overall depth 800mm, width 150mm and total length 2200mm with clear span 2000mm. The numerical model for all beams has shear-span to depth ratio (a/t) =1.0. The cylindrical compressive strength $f_{c'}$ taken 28 MPa and cubic compressive strength f_{cu} is 33 MPa. Figure 5 shows the deflection contours (deformed shape) and the contours of the stresses for all tested beams [1].

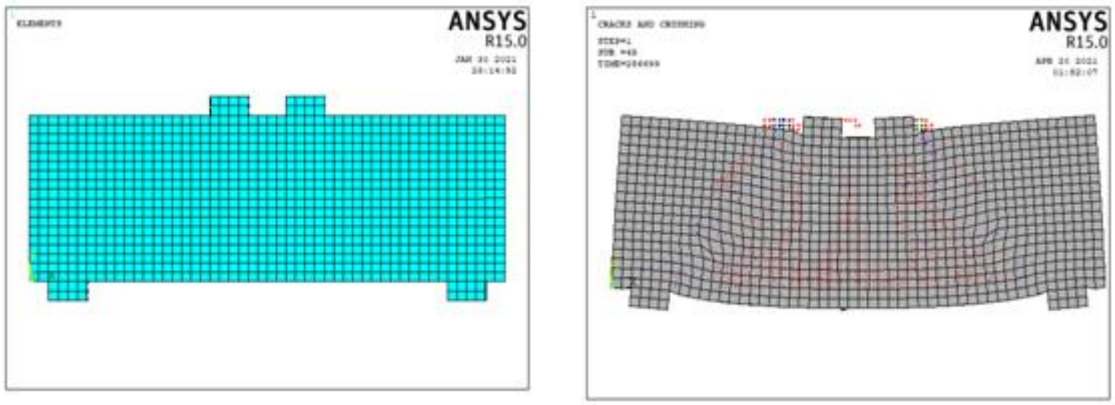

a) Finite element mesh

b) Deformed shape and cracking pattern

Fig 2 Verification model of beam B1 [27]

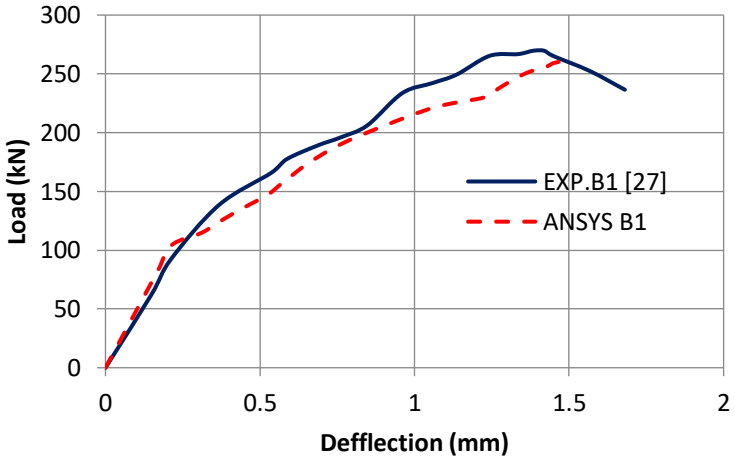

Fig 3 Load-Deflection curve of the verification model [27]

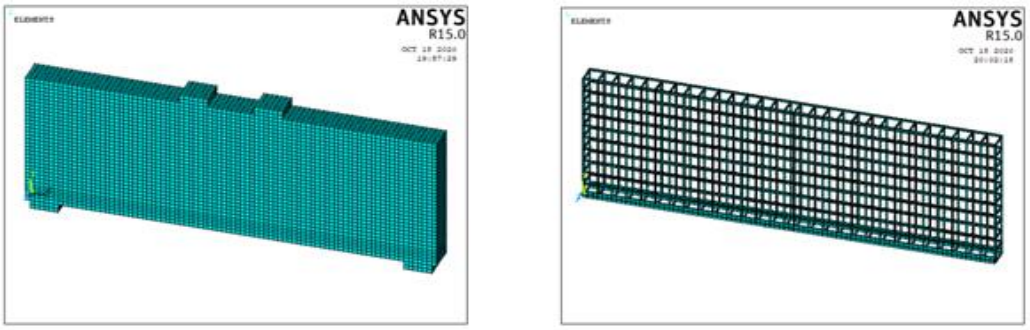

(a) Concrete elements (Solid 65) (b) Reinforcing bar elements (Link 8)

Fig 4 ANSYS idealization for deep beams [1]

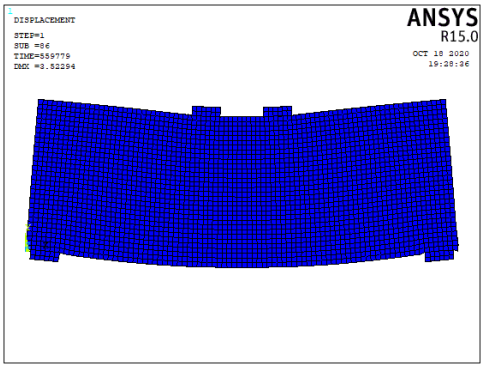

(a) Sample of the deformed shape.

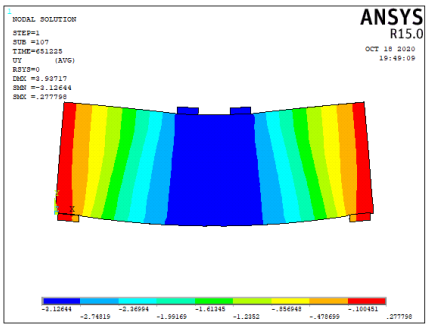

(b) Sample of the deflection contours

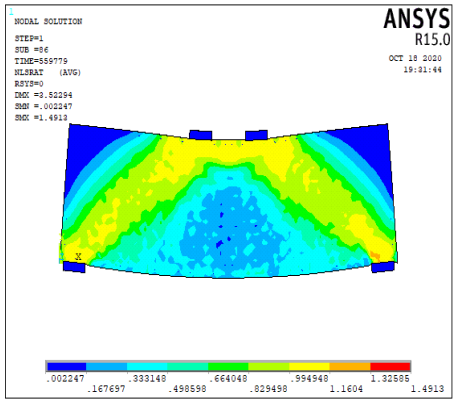

(c) Stress-contours of beam B1

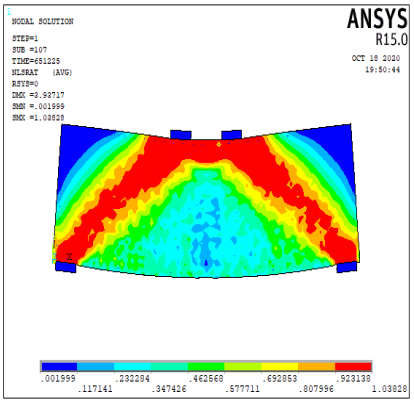

(d) Stress-contours of beam B2

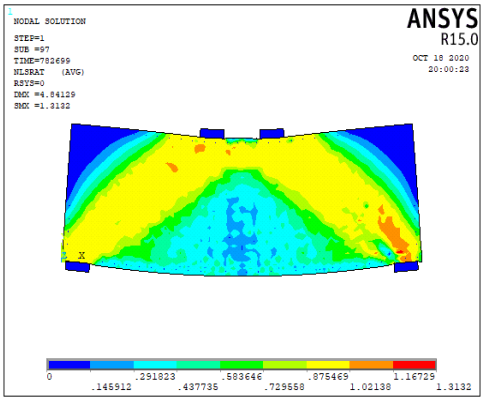

(e) Stress-contours of beam B3

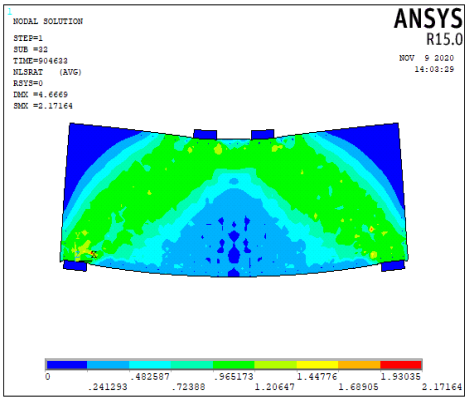

(f) Stress-contours of beam B4

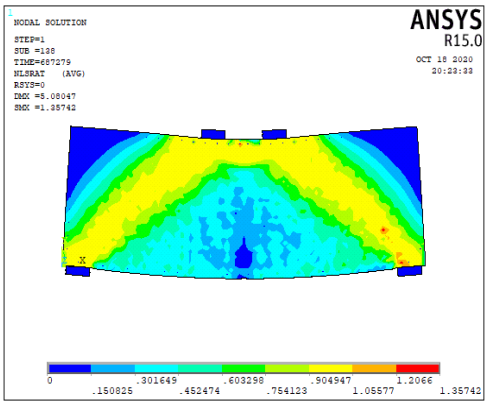

(g) Stress-contours of beam B5

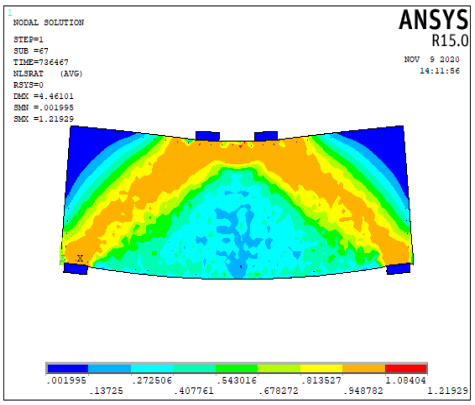

(h) Stress-contours of beam B6

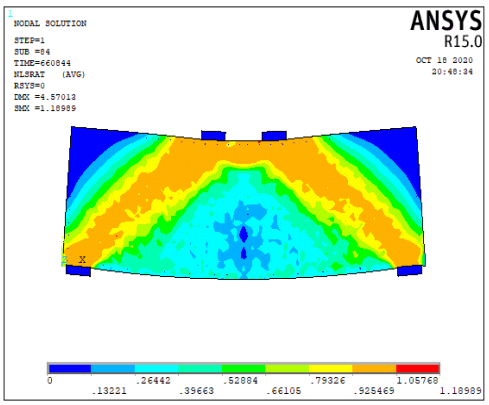

(i) Stress-contours of beam B7

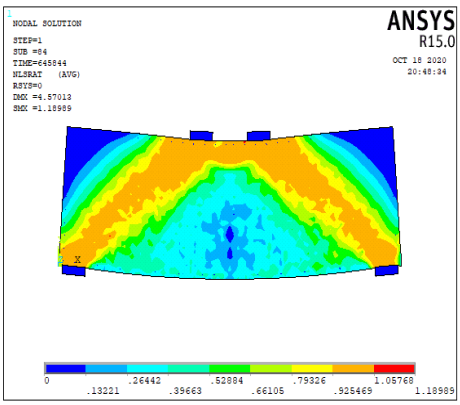

(j) Stress-contours of beam B8

Fig 5 Deformed shapes and stress contours for all tested beams [1]

4.Analysis of Results

The numerical and analytical results from the finite element analysis and STM are shown in Table 1. The numerical results from FE and the experimental results are plotted in Figure 6. Comparison of the experimental, numerical and analytical results shows a good agreement where the mean, standard deviation of the predicted and measured values of the cracking load due to flexure, the cracking load due to shear, the ultimate load and the ultimate deflection (P_{crf}, P_{crs}, P_u and D_u) shown in Table 2 are in the acceptable range. The mean of ($P_{crf\ FE}/P_{crf\ exp.}$), ($P_{crs\ FE}/P_{crs\ exp.}$), ($P_{u\ FE}/P_{u\ exp.}$), ($D_{u\ FE}/D_{u\ exp.}$), ($P_{u\ STM\ [2]}/P_{u\ exp.}$) and ($P_{u\ STM\ [3]}/P_{u\ exp.}$) are 100.44 %, 97.55 %, 102.27 %, 95.70 %, 99.27 % and 99.97 %, respectively. The load-deflection curves for beams B7 and B8 from the numerical results are very similar to that of the experimental ones as shown in Figure 6.g and 7.h. The standard deviation of the loads level stayed under 10. Also Table 2 shows that both the ECP 203-2017 [2] and ACI 318-18 [3] are conservative in calculating the ultimate shear load using STM. However, the ECP 203-2017 [2] is more conservative than ACI 318-18 [3].

Table 1 Predicated results from FE and STM.

Beam	FE				STM	
	$P_{crf\ FE}$ (kN)	$P_{crs\ FE}$ (kN)	$P_{u\ FE}$ (kN)	$\Delta_{u\ FE}$ (mm)	$P_{u\ STM}$ [2] (kN)	$P_{u\ STM}$ [3] (kN)
B1	214.20	287.00	559.70	3.60	519.30	573.30
B2	231.70	291.78	651.20	3.93	613.10	614.20
B3	241.70	311.78	782.70	4.84	847.30	800.50
B4	254.28	358.97	904.00	4.66	1016.80	1030.00
B5	251.70	297.41	687.20	5.08	639.30	634.60
B6	259.28	314.28	736.47	4.46	654.30	643.30
B7	240.50	275.22	660.00	3.79	620.80	622.60
B8	216.00	263.66	638.84	4.56	600.30	614.30

Table 2 Comparison between experimental, numerical and analytical results.

Beam No.	B1	B2	B3	B4	B5	B6	B7	B8	Mean	Standard Deviation
$P_{crf\ FE}$ / $P_{crf\ exp.}$ %	107.10	105.32	96.68	97.80	100.68	96.03	96.20	102.86	100.33	4.07
$P_{crs\ FE}$ / $P_{crs\ exp.}$ %	106.30	97.26	97.43	105.58	95.94	98.21	88.78	90.92	97.55	5.76
$P_{u\ FE}$ / $P_{u\ exp.}$ %	98.96	103.74	98.94	101.57	103.53	103.73	103.13	104.16	102.22	2.02
$D_{u\ FE}$ / $D_{u\ exp}$ %	111.80	94.93	93.80	89.62	87.89	102.53	102.16	98.49	97.65	7.16
$P_{u\ STM\ [2]}$ / $P_{u\ exp.}$ %	91.81	97.67	107.10	114.25	96.31	92.15	97.00	97.88	99.27	7.16
$P_{u\ STM[3]}$ / $P_{u\ exp.}$%	101.36	97.85	101.18	115.73	95.60	90.61	97.28	100.16	99.97	6.80
$P_{uSTM[2]}$/$P_{uSTM[3]}$%	90.58	99.82	105.85	98.72	100.74	101.71	99.71	97.70	99.35	4.03

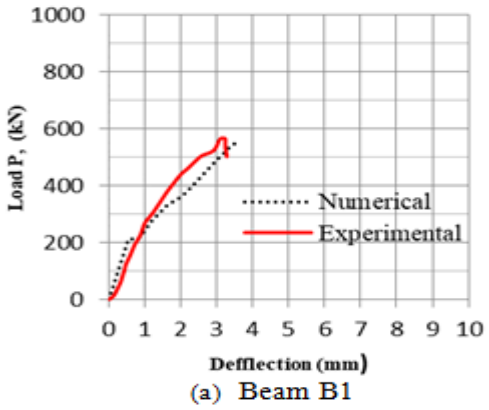

(a) Beam B1

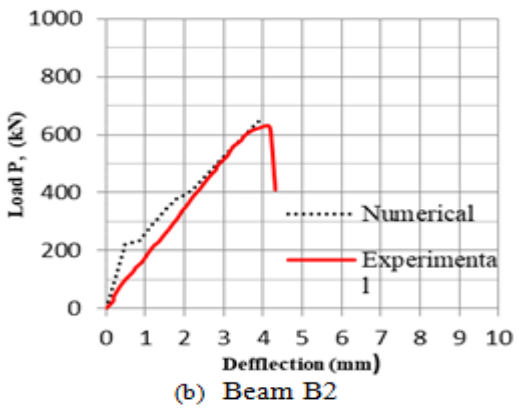

(b) Beam B2

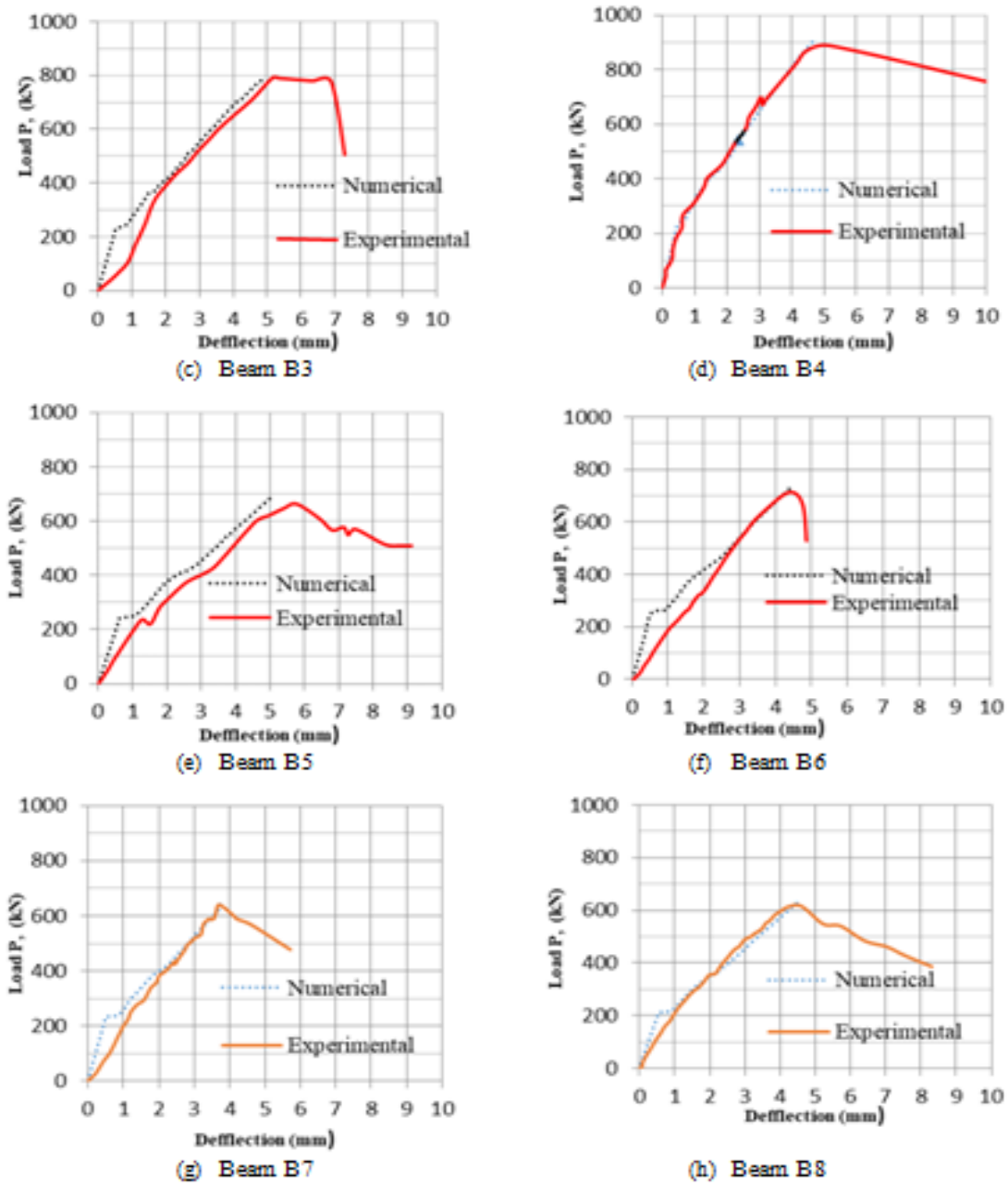

Fig 6 Experimental and numerical load-deflection curves [1]

5. Parametric study

Nine variable parameters are taken into consideration during study full scale deep beam models in the parametric study: (1) concrete compressive strength f_{cu}; (2) reinforcing steel yield strength f_y; (3) beam depth to span ratio (t/L); (4) beam width to span ratio (b/L); (5) shear span to depth ratio (*a/d*); (6) main steel ratio (m/m_{max}); (7) web reinforcement percent (r_s %) ; (8) fiber volumetric percent (V_f %) and (9) fiber aspect ratio (L_f/F_f). All deep beams have an overall length 6500mm with clear span 6000mm. Figure 7 shows the concrete dimensions and reinforcement details for the full scale deep beam used in the parametric study. Figure 8 shows the boundary conditions and the supports used in the finite element model by ANSYS program. The numerical load-deflection curves for all the twenty full scale deep beams are shown in Figure 9. The ultimate shear strength from the numerical analysis illustrated in Table 3.

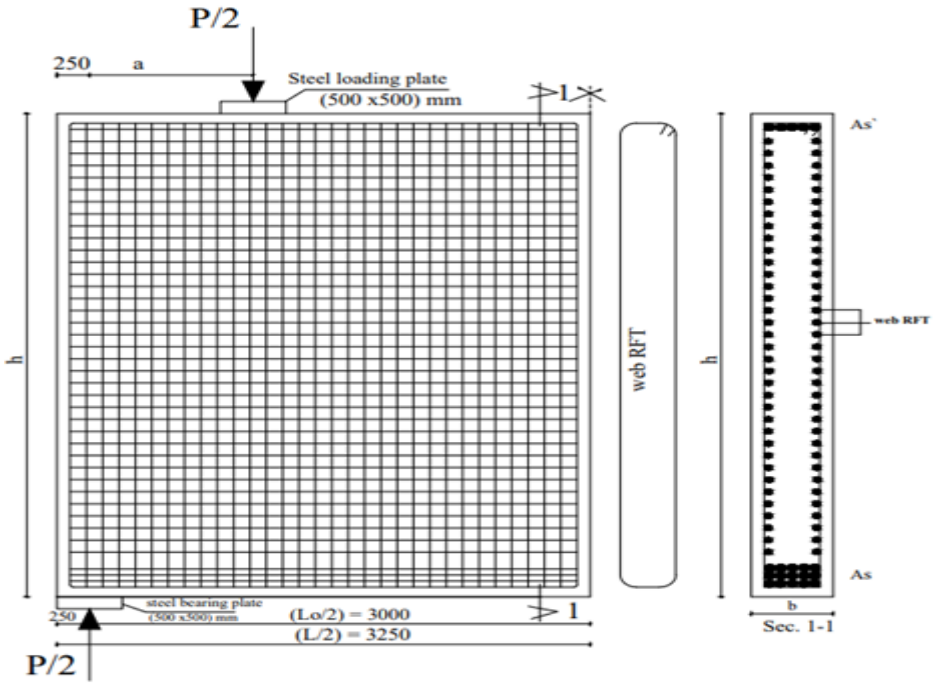

Fig 7 Details of specimen B1 used in the parametric study [1]

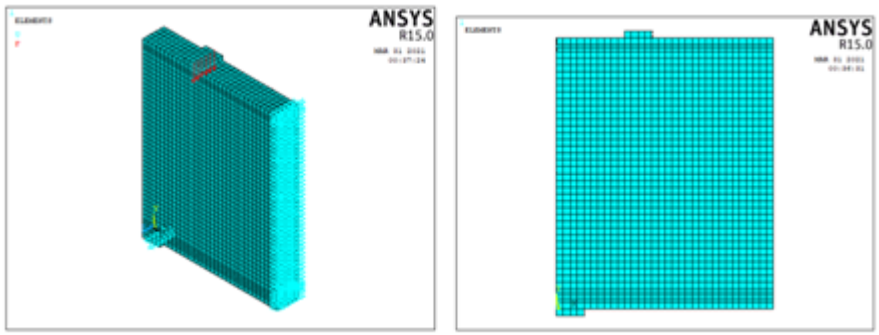

(a) Boundary Conditions and supports **(b) Concrete elements (solid 65)**

Fig 8 Finite element idealization for half deep beam used in the parametric study [1]

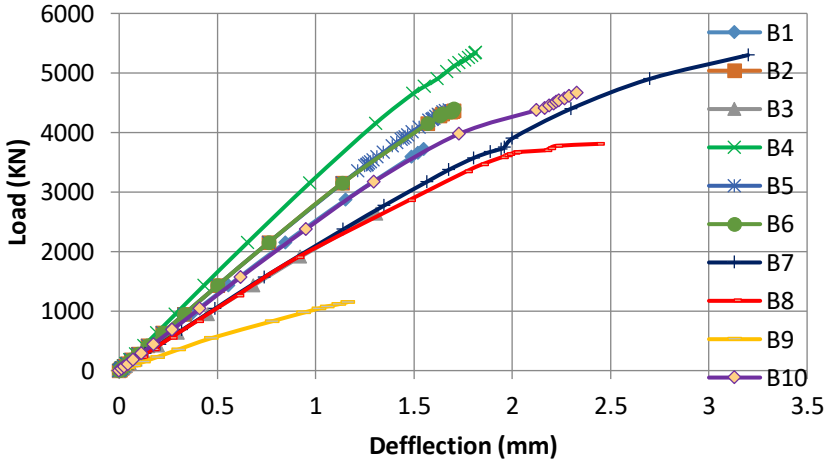

(a) Effect of concrete compressive strength f_{cu}, reinforcing steel yield strength f_y, beam depth to span ratio (t/L), and beam width to span ratio (b/).

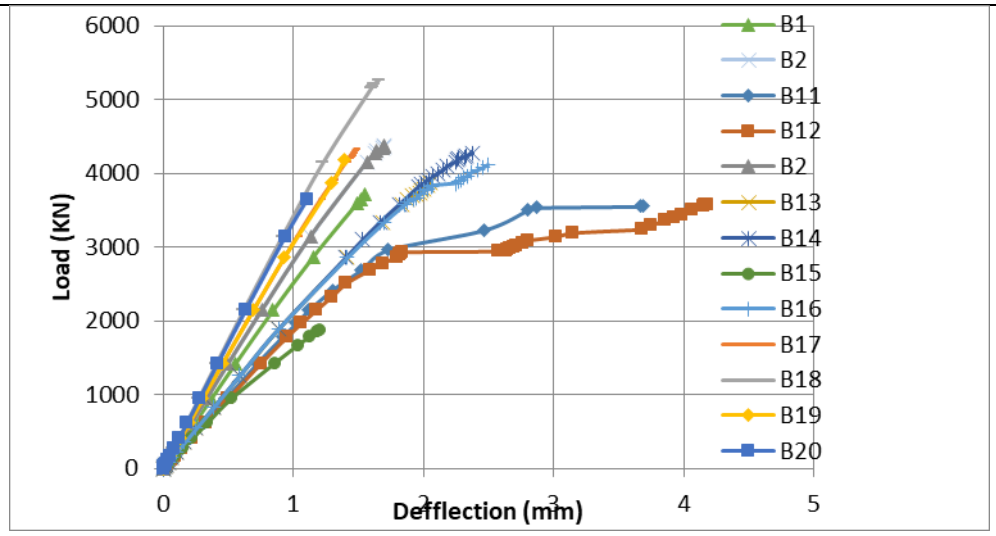

(b) Effect shear span to depth ratio (a/d), main steel ratio (m/m $_{max}$), web reinforcement percent (r_s %) , fiber volumetric percent (V_f %) and fiber aspect ratio (L_f/F_f)

Fig 9 Numerical load-deflection curves for the parametric study [1].

Table 3 The studied parameters and the numerical results from ANSYS program and STM

Beam No.	f_{cu} (MPa)	f_y (MPa)	(t/L)	(b/L)	a/t	μ/μ_{max}	ρ_t (%)	V_f (%)	(L_f/Φ_f)	P_{uFE} (kN)	Δ_{uFE}	$P_{u,STM(2)}/P_{u,FE}$	$P_{u,STM(1)}/P_{u,FE}$	$P_{u,STM(2)}/P_{u,STM(1)}$	*Studied Factors*
1	28	360	0.67	0.083	0.25	0.3	1.00	0	0	3716.6	1.54	1.018	1.092	0.933	without fiber
2	28	360	0.67	0.083	0.25	0.3	1.00	0.4	50	4368.7	1.70	1.032	1.099	0.939	Effect of concrete compressive strength
3	20	360	0.67	0.083	0.25	0.3	1.00	0.4	50	2630.5	1.309	1.129	1.179	0.958	
4	33	360	0.67	0.083	0.25	0.3	1.00	0.4	50	5340	1.814	1.024	1.086	0.943	
5	28	400	0.67	0.083	0.25	0.3	1.00	0.4	50	4372.3	2.20	1.025	1.099	0.934	Effect of reinforcement steel yield strength
6	28	500	0.67	0.083	0.25	0.3	1.00	0.4	50	4398.6	1.60	1.024	1.119	0.916	
7	28	360	0.75	0.083	0.25	0.3	1.00	0.4	50	5347.9	3.20	1.012	1.028	0.985	Effect of depth to span ratio
8	28	360	0.60	0.083	0.25	0.3	1.00	0.4	50	3807.8	2.43	1.168	1.273	0.917	
9	28	360	0.67	0.067	0.25	0.3	1.00	0.4	50	1149.66	1.16	2.566	2.783	0.922	Effect of width to span ratio
10	28	360	0.67	0.100	0.25	0.3	1.00	0.4	50	4667	2.33	1.198	1.268	0.945	
11	28	360	0.67	0.083	0.30	0.3	1.00	0.4	50	3564.8	3.69	1.067	1.136	0.939	Effect of shear span to depth ratio
12	28	360	0.67	0.083	0.35	0.3	1.00	0.4	50	3578.4	4.18	1.132	1.174	0.965	

13	28	360	0.67	0.083	0.25	0.4	1.00	0.4	50	4867.9	2.60	1.109	1.146	0.968	Effect of main reinforcement ratio
14	28	360	0.67	0.083	0.25	0.5	1.00	0.4	50	5267.2	2.90	1.036	1.054	0.983	
15	28	360	0.67	0.083	0.25	0.3	0.80	0.4	50	1879.6	1.21	1.00	1.13	0.895	Effect of web reinforcement percent
16	28	360	0.67	0.083	0.25	0.3	1.25	0.4	50	4109.3	2.49	1.06	1.14	0.928	
17	28	360	0.67	0.083	0.25	0.3	1.00	0.5	50	4531.5	1.50	1.019	1.136	0.896	Effect of fiber volumetric percent
18	28	360	0.67	0.083	0.25	0.3	1.00	0.6	50	5259.3	1.65	1.010	1.031	0.980	
19	28	360	0.67	0.083	0.25	0.3	1.00	0.4	40	4193.4	1.39	1.055	1.126	0.937	Effect of fiber aspect ratio
20	28	360	0.67	0.083	0.25	0.3	1.00	0.4	60	4749.9	2.00	1.020	1.069	0.954	

$$\rho_s = \frac{n * As}{0.2 * b * s} * 100$$

Where:

n : is the number of branches;

A_s : is the area of one branch;

b: is the beam width;

S = S_v: is the spacing between the horizontal stirrups; and

S = S_h: is the spacing between vertical stirrups.

For the studied variables range, the ultimate shear strength increased by 100 %, 0.70 %, 40.4 % and 306 % respectively due to the increase of the concrete compressive strength (f_{cu}), the steel reinforcement yield strength (f_y), the depth to span ratio (t/L), and width to span ratio (b/L) respectively. Also the ultimate shear strength increased by 20.6 %, 118.6 %, 20.39 % and 13.3% respectively due to the increase of the main reinforcement steel ratio (m/m_{max}), the web reinforcement ratio (r_s), the steel fiber volumetric percent ($V_{f\,\%}$), and the fiber aspect ratio (L_f/ F_f) respectively while the ultimate shear strength decreased by 18 % due to increase the shear span to depth ratio (a/t).

Comparison of the numerical from FE and the analytical results using STM shows a good agreement where the mean, standard deviation of the predicted and measured values of shown in Table (5.4) are in the acceptable range. The mean of ($P_{u\ STM\ [2]}/P_{u\ FE.}$) and ($P_{u\ STM\ [3]}/P_{u\ FE}$) are 104 %, and 110 % respectively and the standard deviation of the loads level stayed under 5 %. Also Table (5.4) shows that both the ECP 203-2017 [2] and ACI 318-18 [3] are conservative in calculating the ultimate shear load using STM. The ECP 203-2017 [2] is more conservative than ACI 318-18 [3].

6. Conclusions

1- The comparison between experimental results and nonlinear finite element results using ANSYS program V 15 shows a good agreement, where the mean value of cracking load, ultimate load and displacement at ultimate load is 97.55%, 102.22% and 97.65%, respectively and the standard deviation is less than 6%.

2- The percentage of mean value of the experimental ultimate load to the ultimate load calculating using ECP 203-2017 [2] ($P_{u\ STM\ [1]}/P_{u\ exp.}$) and ACI-218-18 [2] ($P_{u\ STM\ [3]}/P_{u\ exp.}$) is 99.27% and 99.97%, respectively, with standard deviation 7.16% and 6.80% which means that both the Egyptian and American codes are conservative and the Egyptian code is more conservative than the American code.

3- Main reinforcement steel ratio and steel fiber volumetric percentage has significant effect on the cracking load, ultimate load, displacement ductility and toughness of the reinforced concrete lightweight deep beams.

4- Increasing the main reinforcement ratio by 33 % and 66 % increases the cracking load by 14 % and 18 %, the ultimate load by 26 % and 42 %, the displacement ductility by 24 % and 31 % and the toughness by 45 % and 92 % respectively.

5- From the nonlinear finite element analysis using ANSYS program , best predictions of the modified strut and tie model (MSTM) are obtained as a result of the parametric study for the following factors: (1) concrete compressive strength (f_{cu}) 20,25,28, and 33 MPa, (2) steel yield strength (f_y) 360,400 and 500 MPa, (3) depth to span ratio (t/L) 0.6,0.67 and 0.75, (4) width to depth ratio (b/t) 0.067,0.083 and 0.1, (5) shear span-to-span ratio (*a/L)* 0.25,0.3 and 0.35, (6) main steel ratio (m /m $_{max}$) 0.30, 0.4 and 0.5, (7) percentage of stirrups (r_s %) 0.8,1.0 and 1.25, (8) steel fiber volumetric percent (V_f) % = 0, 0.4,0.5 and 0.6 , and (9) steel fiber aspect ratio (l_f / ϕ_f) 40, 50 and 60.

REFERENCES

[1] Manharawy, M.S." Behavior of structural lightweight reinforced concrete deep beam with steel fiber", M.Sc., Faculty of Engineering, Shoubra, Benha University, 2021.

[2] Egyptian Code of Practice for Design and Construction of Reinforced Concrete Structures ECP-203, Housing and Building Research Center, Ministry of Building and Construction, Giza, Egypt, 2017, Chapter 6, pp. 113-122.

[3] ACI Committee 318-18, Building Code Required for Reinforced Concrete, (ACI 318-18) and Commentary (ACI 318R-18), American Concrete Institute, Farmington Hills, Mich,2018.

[4] AL-Kasasbeh, T., and Allouzi, R., "Behavior of polypropylene fiber reinforced foamed concrete beams laterally reinforced with/without glass fiber grid", International Journal of Structural Integrity, 9864-1757, 2020.

[5] Mohamed, A., El Madawy, M.E., Chung, S.Y., Sikora, P. and Stephan, D., "Preparation and characterization of ultra-lightweight foamed concrete incorporating lightweight aggregates", Journal of Applied Sciences 9.7, 1447, 2019.

[6] Lim, S.K., Tan, C.S., Li, B., Ling, T., Hossain, M.U. and Poon, C.S., "Utilizing high volumes of quarry wastes in the production of lightweight foamed concrete", Journal of Construction Building Materials, 2017, 151, 441–448.

[7] Hilal, A.A., Thom, N.H., and Dawson, A.R., "On void structure and strength of foamed concrete made without/with additives", Journal of Construction and Building. Materials, 85, 157–164, 2015.

[8] Humnabad, A. N., and Autade, P.B., "Experimental evaluation shear strength of steel fiber reinforced concrete deep beams", International Journal of Engineering Research and Technology (IJERT) 5.05, 2016.

[9] Mohamed, K., Farghaly, A.S. and Benmokrane, B., "Proposed strut-and-tie model for concrete deep beams reinforced with FRP bars", Canada Research Chair in Advanced Composite Materials for Civil Structures, June 1–4, 2016.

[10] Vilar, M.M.S., Sartorato, M., Santana, H.B. and Leite, M.R., "Finite elements numerical solution of deep beams based on layer wise displacement field", Journal of the Brazilian Society of Mechanical Sciences and Engineering, 40.9, 477, 2018.

[11] Abhijeet, P., and Mehetre, A.J., "Evaluation of effectiveness of SFRC deep beams in shear", International Journal of Research Studies in Science, Engineering and Technology, Vol. 2, No. 7, 2015.

[12] Ganesan, N., and Indira, P.V., "Engineering properties of steel fiber reinforced geopolymer concrete", Journal of Advances in Concrete Construction 1.4, pp. 305,2013.

[13] Balgude, M.R. and Vijaysinh, V., "Experimental study on crimped steel fiber reinforced concrete deep beams in shear", IOSR Journal of Mechanical and Civil Engineering 11.2, pp. 24-39,2014.

[14] Nipurte, O., Patil, L., Patil, P. and Potinda, V., "Study of behavior of steel fiber reinforced concrete in deep beams for flexure", IJSRSET, International Journal of Scientific Research in Science, Engineering and Technology, ISSN: 2395-4099, Vol. 4, No. 1, 2018.

[15] Magdalene, P.S. and Kanmani, V., "Experimental and numerical study of deep beams by finite element method (FEM)", Journal of Engineering Research and Application, ISSN: 2248-9622, Vol. 8, No.7 (Part-II), 2018.

[16] Santos, D. P., Neto, F., Reginato,J.A.D., and Carrazedo, R. I., "Optimized design of RC deep beams based on performance metrics applied to strut and tie model and in-plane stress conditions", Latin American Journal of Solids and Structures, 16.7 ,2019.

[17] Agus, S., and Taufik, S., "Numerical modelling behavior of reinforced concrete deep beams with strut-and-tie model", International Journal of Mechanical Applications, Vol. 8, pp. 1-9, 2008

[18] Aaron, C.B., Wilson, K. E., Bayrak, O., and Russo, F.M., "Strut-and-tie modeling (STM) for concrete structures, design examples", FHWA-NHI-17-071, National Highway Institute (US), 2017.

[19] Mohammad, P., Chai, H.K., and Voo, Y.L., "Refinement of strut-and-tie model for reinforced concrete deep beams", Plos One, June 25, 2015, https://doi.org/10.1371/Journal.pone.0130734.

[20] Adnan, A.A., and Khadhim, A.M., "Studying the behavior of lightweight deep beams with openings", International Journal of Engineering Technologies and Management Research, 6.12, pp. 89-100, 2019.

[21] Karolína, T., "Tow parameters kinematic approach for the shear behavior of deep beams made of fiber-reinforced concrete", Master Theses, Faculty of Sciences Applications, European Mundus - 11134, 528,2017.

[22] Taufik, S., Anggarini.E. and Setiawan, I.,"ANSYS numerical modeling of confined deep beams with high strength concrete", International Journal of Structural Glass and Advanced Materials Research, Vol. 4: pp. 41.55, 2020.

[23] Douread, R.H., Samad, A. A. A., Mohamad, N., Attiyah, A. N., Mezher, T. M., and Azeez, A. A, "Nonlinear analysis of RC deep beams strengthened with NSM CFRP anchor bars", International Journal of Advanced and Applied Sciences, 5.11, pp. 61-66, 2018.

[24] Mohammad, M., Zarrini, M., Farsangi, N., E., and Gerayli, N., K., "Prediction of structural response for HSSCC deep beams implementing a machine learning approach", International Journal of Coastal and Offshore Engineering, 2.1, pp. 35-43, 2018.

[25] Sri, H.G., and Raju, P.P., "Shear strength of deep beams: a state of Art", International Conference on Advances in Civil Engineering (ICACE-2019), Vol. 21, 2019.

[26] Thomas, P. and Tharu, B., "Analytical study on lightweight concrete deep beams", Journal of Transactions on Engineering and Sciences, ISSN: 2347-1964, Vol.2, No. 10, 2014.

[27] Adam, M. A., Said, M., and Elrakib, T. M., "Shear performance of fiber reinforced self-compacting concrete deep beams", International. Journal of Civil Engineering Technology, (IJCIET), Vol. 7, No.1, pp. 25-46, 2016.